Journal of Alloys and Compounds 495 (2010) 72–75

Contents lists available at ScienceDirect

Journal of Alloys and Compounds

journal homepage: www.elsevier.com/locate/jallcom

A transparent surface-crystallized Eu^{2+}, Dy^{3+} co-doped strontium aluminate long-lasting phosphorescent glass-ceramic

Liyuan Xiao, Qin Xiao, Yingliang Liu*, Pengfei Ai, Yidong Li, Houjin Wang

Department of Chemistry, Jinan University, Guangzhou 510632, People's Republic of China

ARTICLE INFO

Article history:
Received 7 November 2009
Received in revised form
15 December 2009
Accepted 18 December 2009
Available online 28 December 2009

Keywords:
Long lasting phosphorescence
Glass-ceramic
Strontium aluminate
Surface-crystallized

ABSTRACT

A high-brightness Eu^{2+} and Dy^{3+} co-doped strontium aluminate-based transparent surface-crystallized long-lasting phosphorescent (LLP) glass-ceramic was synthesized using solid-state sintering method in CO atmosphere. The crystal structure, morphology and optical properties of the composite were characterized. By the X-ray diffraction diffusion (XRD) data, $SrAl_2O_4$ was demonstrated to be the crystallite in the glass-ceramic. The TEM photographs indicated that the sample had a universal small crystallite size about 10–20 nm on its surface. The $SrAl_2O_4$:Eu^{2+}, Dy^{3+} crystallites were produced during the quenching process. After irradiated with ultraviolet (UV) light, the glass-ceramic emitted green long-lasting phosphorescence with an excitation peak at 375 nm and emission peak at 520 nm ascribed to the characteristic 5d–4f transition of Eu^{2+}. Both the PL spectra and luminance decay revealed that this phosphor had efficient luminescence and long-lasting properties. By comparing with the heat-treated sample, the obtained transparent surface-crystallized LLP glass-ceramic puts up higher transparency and long phosphorescence, and could be obtained more easily.

1. Introduction

Rare earth-doped glasses in recent years find enhanced interest due to their potential application in fiber amplifiers, lasers, fluorescent devices and white light emitting diode (LED) [1–4]. Nevertheless, the weak luminescence properties of glass limited their further application for the optical devices [5]. Glass-ceramic, as the glass and crystal composite, has attracted strong interests for its excellent luminescence properties, machinability, high uniformity and stability [6,7].

Glass-ceramics are usually prepared by controlled nucleation and crystallisation of precursor glass (as-melted) at temperature region slightly above the glass transformation temperature, Tg, to obtain the nanocrystalline phase around the rare earth impurity [8]. However, it is difficult to control such heat-treatment process precisely. In numerous LLP glass-ceramic systems, borate glass is one of the best choices for its low melting point, high thermal stability and good rare earth ions solubility [9,10,11]. The $SrAl_2O_4$:Eu^{2+}, Dy^{3+} phosphor, which has more significant advantages than traditional sulfide phosphors, including high brightness, good chemical durability, slow fading and lack of radioactive materials, has received rapidly growing interests, especially some other rare earth-doped alkaline-earth aluminates-based LLP materials.

In this article, a high-brightness transparent surface-crystallized Eu^{2+} and Dy^{3+} co-doped strontium aluminoborate glass-ceramic has been prepared using solid state sintering method. In comparison with the transparent glass via polishing and the heat-treated $SrAl_2O_4$:Eu^{2+}, Dy^{3+} LLP glass-ceramic, the homogeneous surface-crystallized glass-ceramic can be formed by a sample method and shows some advantages.

2. Experimental details

Analytic-grade $SrCO_3$, Al_2O_3, H_3BO_3, Eu_2O_3 (99.99%), Dy_2O_3 (99.99%) were used as starting materials. The batches were weighted with the molar ratio $50\%SrCO_3-(27+x)\%Al_2O_3-(23-x)\%B_2O_3-0.01(27+x)\%Eu_2O_3-0.02(27+x)\%Dy_2O_3$ ($x = 1–10$). The well-mixed batches were put into a small alumina crucible and covered. Then, the small crucible was placed into a larger alumina crucible and covered. Some active carbon granules were loaded in the large crucible to obtain a reducing atmosphere to prevent the oxidation of Eu^{2+} ions during melting. After heated at 1300–1600 °C for 1 h in an electric furnace, the melts were poured into a stainless-steel mold and quenched at room temperature. It does not require a separate crystallization process. However, low-temperature annealing with CO as protective atmosphere to avoid the oxidation of Eu^{2+} is necessary to decrease stress in the glass.

The surface-crystallized $SrAl_2O_4$: Eu^{2+}, Dy^{3+} LLP glass-ceramics (SABED) with green LLP properties were obtained after annealing at 500 °C for 6 h. The crystalline phase of the LLP glass-ceramics is formed during the cooling process. The surfaces of the LLP glass-ceramics were mechanically polished to remove the crystalline phase completely and to obtain a mirror surface glass (SABED-P).

SABED was heat treated at 770 °C for nucleation for 3 h and 792 °C for crystallization for 2 h with CO as protective atmosphere to obtain devitrified glass (SABED-H). (The temperatures of glass transition Tg and crystallization peak Tp of SABED glass-ceramic were determined as 726 and 792 °C by TG-DSC operated at a heating rate of 10 K/min, respectively).

---

* Corresponding author. Tel.: +86 20 85221813; fax: +86 20 85221697.
E-mail address: tliuyl@jnu.edu.cn (Y. Liu).

0925-8388/$ – see front matter © 2010 Published by Elsevier B.V.
doi:10.1016/j.jallcom.2009.12.118

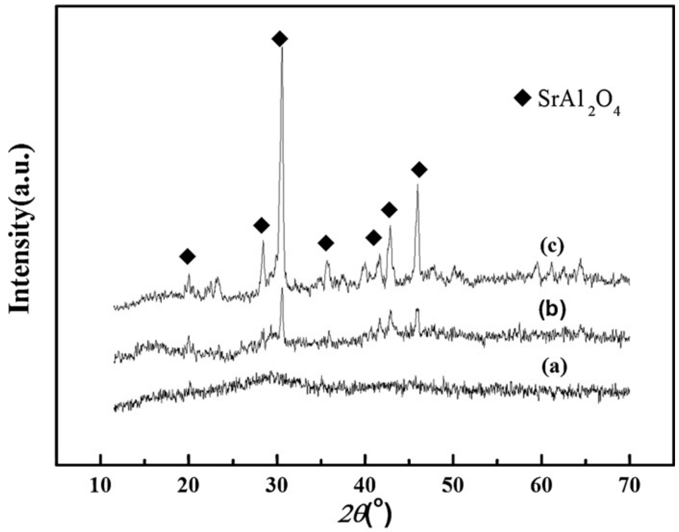

Fig. 1. XRD patterns for the surface of (a): $SrAl_2O_4$: Eu^{2+}, Dy^{3+} glass-ceramic via polishing (SABED-P); (b): $SrAl_2O_4$: Eu^{2+}, Dy^{3+} LLP glass-ceramic (SABED); (c): Heat-treated $SrAl_2O_4$: Eu^{2+}, Dy^{3+} LLP glass-ceramic (SABED-H).

The structures of the samples were determined by a Rigaku Model D/max-II B X-ray diffractometer with Cu Kα_1 (λ = 0.15405 nm) radiation at a 0.02° (2θ) min^{-1} scanning step. The microstructures of obtained glass-ceramics were observed by transmission electron microscopy (TEM, Philips TECNAI 10). The photoluminescence spectra and intensity were measured on Hitachi F-4500 spectra fluorescence spectrophotometer (150W Xe lamp and grating monochromator). The thermoluminescence (TL) spectra were measured by FJ427A1 (China) in the temperature range of 30–300 °C at a heating rate of 2 °C/s. All measurements were carried out at room temperature expect for the TL spectra.

3. Results and discussion

3.1. Crystal structures of the synthesized samples

The crystal structures of the synthesized samples are checked, as shown in Fig. 1. Fig. 1(b) shows that the crystalline phase in the LLP glass-ceramic is monoclinic $SrAl_2O_4$, the XRD data matches well with powder diffraction file no. 34-0379 (International Centre for Diffraction Data, Newtown Square, PA.). No XRD peaks are detected in Fig. 1(a), which indicates that the crystallization of SABED occurred only on the glass surfaces. We can see clearly that the intensity of diffraction peaks increases significantly from SABED-P to SABED-H in Fig. 1. However, the three strongest peaks located at 28°–30° changed into broad reflections caused by the existence of an amorphous phase. The crystallinities of the samples are lower than that of the monocrystalline $SrAl_2O_4$ power, which is also a main reason for such broad reflections.

3.2. The microstructures of the obtained glass-ceramics

Fig. 2 portrays TEM photographs of $SrAl_2O_4$: Eu^{2+}, Dy^{3+} LLP glass via polishing (a), $SrAl_2O_4$: Eu^{2+}, Dy^{3+} LLP glass-ceramic (b) and the opaque heat-treated ceramic (c). In contrast to Fig. 2(b) and Fig. 2(c), we cannot see any crystalline grain in Fig. 2(a) except amorphous glass phase. It indicates that the crystallization of the SABED is occurring on the surface. It is observed that the obtained LLP glass-ceramic is surface-crystallized and has a universal crystallite size about 10–20 nm (Fig. 2(b)). The crystalline grains disperse well on the surface of SABED. There are several defaults on the surface which can provide vacancies for the growing of crystalline. The impurities and defaults on the surface of the glass can also decrease the crystallization activation energy and the stability of the glass.

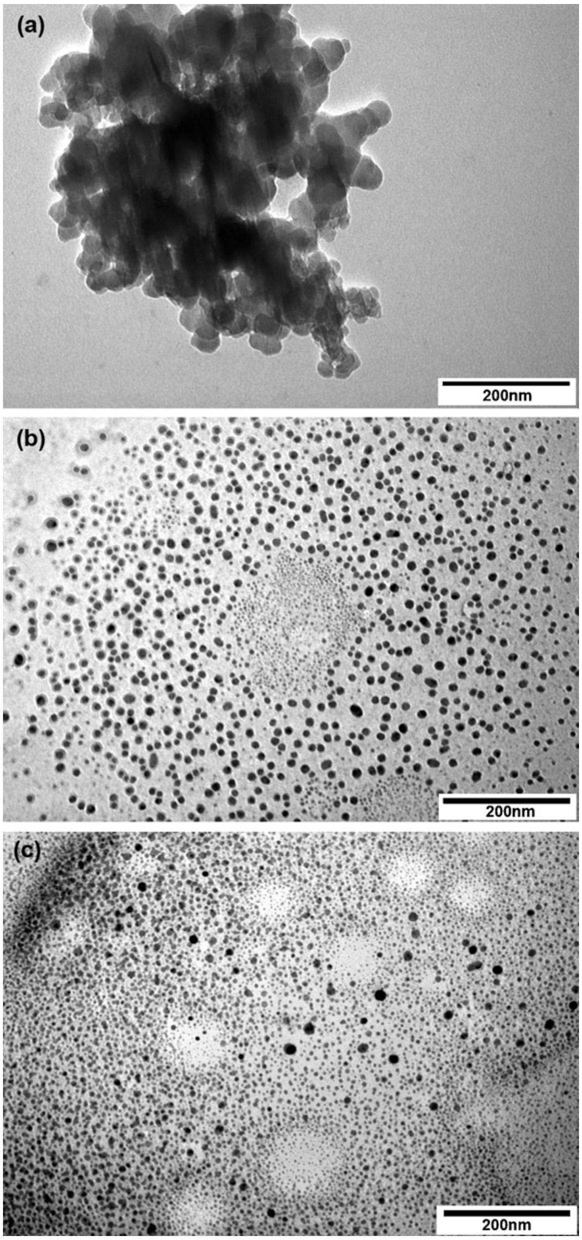

Fig. 2. TEM photographs of (a): SABED-P; (b): SABED; (c): SABED-H.

It also can be seen from Fig. 2(b) that there are some places with crystallite size less than 5 nm. The reason of such phenomenon can be regarded as an asymmetrical quenching process when pouring the melts into a stainless-steel mold. Parts of the crystallites which expose in air or contact with the cool stainless-steel mold quench faster than those not exposed. However, such fast quenching process goes against with the growing of crystallites, so that these crystallites keep lesser size.Fig. 2(c) shows the distribution of the crystalline grains of devitrified glass (SABED-H). The crystalline grains dispersed densely and spread all over the sample. In contrast with the sample obtained by heat-treatment, crystalline grains of the surface-crystallization sample dispersed more evenly on the surfaces.

3.3. Luminescence properties of synthesized glass-ceramics

Excitation and emission spectra of synthesized glass-ceramics have been measured (Fig. 3). The excitation spectra of three samples show very strong absorption in the band from 300 to 450 nm with a peak at 375 nm, which means it can be excited effectively

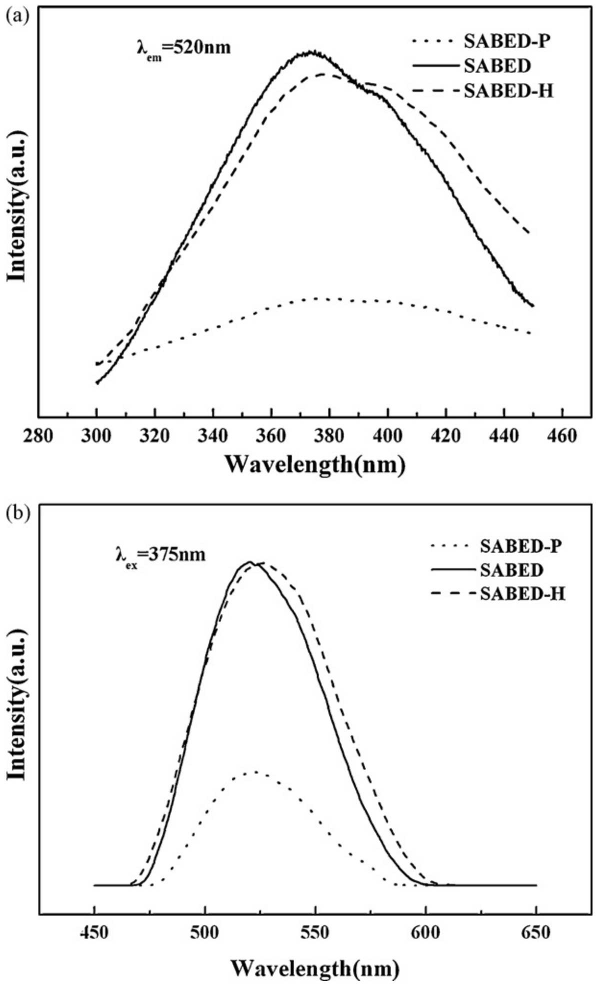

Fig. 3. Excitation spectra (a) and emission spectra (b) of SABED-P, SABED and SABED-H.

by ultraviolet light, sunlight and fluorescence. For all the known LLP materials, Eu^{2+} is the most important activation ion. Because the 5d electron of Eu^{2+} is strongly coupled with the lattice of the host, the phosphorescence of Eu^{2+} usually changes with its host, for example, red emission in CaS [12], green in $SrAl_2O_4$ [13] and blue in $CaAl_2O_4$ [6,13]. The same interpretation is rational for the red shift of the excitation of Eu^{2+} from $SrAl_2O_4$: Eu^{2+}, Dy^{3+} powder sample obtained by solid-state reaction (peaking at 350 nm) to glass-ceramic (at 375 nm). It can also be observed that the $SrAl_2O_4$: Eu^{2+}, Dy^{3+} glass-ceramic possesses higher excitation energy than that of the powder sample.

The emission spectra of the glass-ceramics are similar to the emission spectra of $SrAl_2O_4$: Eu^{2+}, Dy^{3+} powder materials. They show a wide band from 450 to 650 nm and a peak at 520 nm (green emission). This emission peak is attributed to the $4f^65d^1$–$4f^7(^8S_{7/2})$ transition of Eu^{2+}. This means that the active carbon can effectively reduce the Eu^{3+} to Eu^{2+}. The Eu^{2+} ions are the luminescence centers for the phosphorescence.

In contrast with the SABED, the PL peaks of SABED-H shift to longer wavelength. This slight red shift may be caused by changes of the crystal field around Eu^{2+} ions [14]. The PL intensity of SABED-P is lower than SABED and SABED-H, it can also be attributed to the change of the lattice of the host.

3.4. *Afterglow decay curves of synthesized glass-ceramics*

Fig. 4 shows the afterglow decay curves of SABED, SABED-H and SABED-P at room temperature after excited by UV-light for 100 s. The decay curves of SABED and SABED-H indicate that the decay process contains a rapid-decaying and a slow-decaying process. However, SABED-P has no LLP phenomenon. The absence of afterglow in the case of SABED-P indicates that the presence of $SrAl_2O_4$ crystallines is necessary for retaining long persistence.

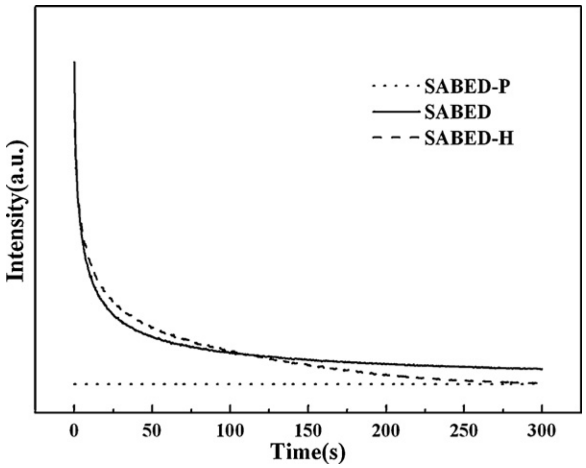

Fig. 4. Afterglow decay curves of SABED-P, SABED and SABED-H.

The phosphorescence characteristics are evaluated based on the decay times that have been calculated using a curve fitting technique. The decay curves are fitted using the equation [15]:

$$I = I_0 + a_1 \ \exp(-t/\tau_1) + a_2 \ \exp(-t/\tau_2) \tag{1}$$

where I is the phosphorescence intensity at any time 't' after switching off the excitation illumination, α_1 and α_2 are constants, and τ_1 and τ_2 are decay times for exponential components, respectively. Decay curves are fitted by the sum of two exponential components having different decay times: initial rapid decay corresponding to the intrinsic lifetime of Eu^{2+}, followed by the long decay of the afterglow due to thermal trapping–detrapping of charge carriers. The values of τ_1 and τ_2 of the LLP glass-ceramics are obtained, as listed in Table 1. The results illustrate that both SABED and SABED-H show a rapid decay, and then long-lasting phosphorescence. Both τ_1 and τ_2 of SABED are larger than that of SABED-H, which may be caused by defect sizes [16,17,18].

The phosphorescence characteristic of Eu^{2+} and Dy^{3+} co-activated strontium aluminates glass-ceramics has been explained after many investigations had been proposed. Some researchers submit a mechanism in which it is inferred that Eu^{2+} is reduced into Eu^+ and Dy^{3+} is oxidized into Dy^{4+} during the excitation, respectively [13]. Aitasalo [19] proposed several different viewpoints: Besides the uncertainty of the existence of Eu^+, it was difficult to reduce the Eu^{2+} into Eu^+ and oxidize the Dy^{3+} into Dy^{4+} on treatment with just the irradiation of the UV or visible light. Clabau [20] summed up the phosphorescence mechanism of $SrAl_2O_4$:Eu^{2+},Dy^{3+} LLP materials as follows: Electrons are promoted from the occupied 4f levels of Eu^{2+} to the empty 5d levels and the conduction band (CB) under UV irradiation, parts of them are trapped at the oxygen vacancy levels V_O located in the vicinity of the photo-generated Eu^{3+} cations. Typically, the oxygen vacancy levels in $SrAl_2O_4$ would correspond to the empty sp^3-orbitals of the Al^{3+} ions (at tetrahedral sites in the perfect solid) surrounding the oxygen vacancy.

Table 1
Decay times of SABED-P, SABED and SABED-H.

Compounds	Decay lifetime(s)	
	τ_1	τ_2
SABED-P	–	–
SABED	7.9	173.3
SABED-H	5.7	81.8

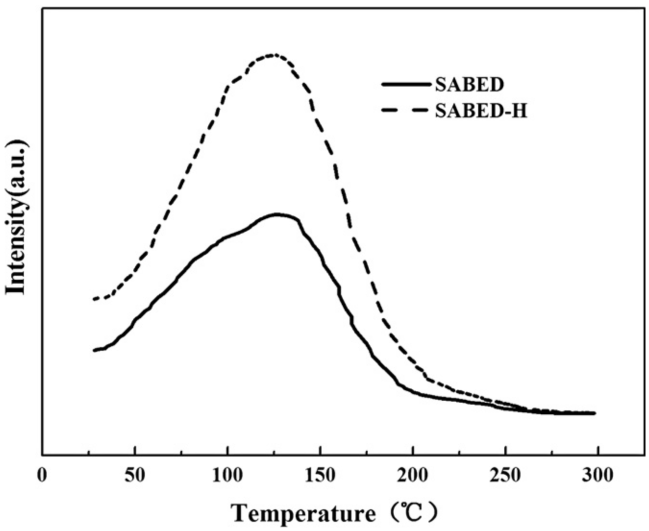

Fig. 5. Thermoluminescence glow curves of SABED and SABED-H.

Although different opinions exist on the mechanism, it is a common viewpoint that energy of the incident light is stored in the form of captured electrons and holes during the excitation part. The captured electrons and holes can be thermally released from the traps at room temperature. The characteristic emission of the luminescence ions can be formed by the subsequent recombination with each other for setting free the energy, such as Eu^{2+}, for the release of the captured electrons and traps is durative, the luminescence of the materials shows the long-lasting property [6].

3.5. Thermoluminescence for the synthesized LLP glass-ceramics

In order to investigate the long phosphorescence of the synthesized LLP glass-ceramics, measurements of the TL glow curves of the samples were carried out. The trap energy level can be estimated using the following half peak width method [21]:

$$E = \frac{2k(T_m)^2}{(T_2 - T_m)} \qquad (2)$$

where k is the Boltzmann's constant; T_m the temperature value corresponding to the peak of the thermo-luminescent curve; T_2 the temperature value corresponding to the point on the right side of the thermo-luminescent curve, where the peak intensity is half of the peak value. The TL curves of SABED and SABED-H which have similar broad bands (Fig. 5), with the maximum peaks at 128 °C and 125 °C, correspond to the trap depths of 0.76 eV and 0.74 eV, respectively. Namely, E values lower than 0.2 eV lead to fast de-trapping at room temperature and prevent a long afterglow, while E values higher than 1.5 eV require annealing at high temperature or laser light to de-trap charge carriers as observed in photostimulable phosphors [22].

It has been known that the trap levels located at a suitable depth have an effective afterglow, and the results are in agreement with Table 1. The subtle difference of TL maxima between SABED and SABED-H indicates that the trapping level of SABED (0.76 eV) is located more deeply than that of SABED-H (0.74 eV), and is also evident from the afterglow decay curves. Hence, it can be concluded that SABED gives higher long phosphorescence than SABED-H.

4. Conclusions

Eu^{2+} and Dy^{3+} co-doped transparent surface-crystallized glass-ceramics (SABED) that contain $SrAl_2O_4$ phases have been prepared without a heat-treatment process. The microcrystalline phase with a crystalline size about 10–20 nm dispersed well on the surface of the glass-ceramic, which was proved to be responsible for the LLP. Green phosphorescence that was due to the $4f^65d$–$4f^7$ transition of Eu^{2+} ions was clearly observed from the SABED glass-ceramic. Compared with the heat-treated sample, the obtained transparent surface-crystallized LLP glass-ceramic has higher transparency and longer phosphorescence, and can be obtained more easily.

The influences of the different preparation conditions on the photoluminescence and afterglow properties still need further study. This high-brightness transparent glass-ceramic has potential application for night display. It also has many advantages compared with powder materials, and has great potential application in LED systems.

Acknowledgments

This present work was financially supported by the National Natural Science Foundations of China (No. 20671042, 50872045) and the Natural Science Foundations of Guangdong Province (No. 05200555, 7005918).

References

[1] K.Y. Jung, H.W. Lee, H.K. Jung, Chem. Mater. 18 (2006) 2249–2255.
[2] T. Hayakawa, M. Hayakawa, M. Nogami, J. Alloys Compd. 451 (2008) 77–80.
[3] D. Jin, R. Connally, J. Piper, J. Phys. D: Appl. Phys. 39 (2006) 461–465.
[4] J.L. Doualan, P. Camy, R. Moncorge′, E. Daran, M. Couchaud, B. Ferrand, J. Fluorine Chem. 128 (2007) 459–464.
[5] J.S. Cheng, P.J. Tian, W.H. Zheng, J. Xie, Z.X. Chen, J. Alloys Compd. 471 (2009) 470–473.
[6] C.Y. Li, Q. Su, J. Alloys Compd. 408–412 (2006) 875–878.
[7] J. Fu, J.M. Parker, P.S. Flower, R.M. Brown, Mater. Res. Bull. 37 (2002) 1843–1849.
[8] G. Dominiak-Dzik, W. Ryba-Romanowski, J. Alloys Compd. 451 (2008) 586–590.
[9] H. Lin, E.Y.B. Pun, X.J. Wang, X.R. Liu, J. Alloys Compd. 390 (2005) 197–201.
[10] J. Pisarska, J. Phys. Condens. Matter 21 (2009) 285101/1–285101/6.
[11] M.A.K. EI-Fayoumi, M. Farouk, J. Alloys Compd. 482 (2009) 356–360.
[12] D. Jia, W. Jia, D.R. Evans, W.M. Dennis, H. Liu, J. Zhu, W.M. Yen, J. Appl. Phys. 88 (2000) 3402–3407.
[13] T. Matsuzawa, Y. Aoki, N. Takeuchi, T. Murayama, J. Electrochem. Soc. 143 (1996) 2670–2673.
[14] B.S. Feng, J.C. Zhang, L. Song, X.Y. Yu, Am. Ceram. Soc. Bull. 87 (2008) 53–55.
[15] A. Nag, T.R.N. Kutty, J. Alloys Compd. 354 (2003) 221–231.
[16] X.D. Lü, M.J. Zhong, R.Q. Wang, J. Wuhan Univ. Technol. 23 (2008) 652–657.
[17] C.K. Chang, L. Jiang, D.L. Mao, C.L. Feng, Ceram. Int. 30 (2004) 285–290.
[18] Y.H. Lin, Z.L. Tang, Z.T. Zhang, C.W. Nan, J. Alloys Compd. 348 (2003) 76–79.
[19] T. Aitasalo, J. Hölsä, H. Jungner, M. Lastusaari, J. Niittykoski, J. Lumin. 94/95 (2001) 59–63.
[20] F. Clabau, X. Rocquefelte, S. Jobic, P. Deniard, M.-H. Whangbo, A. Garcia, T. Le Mercier, Chem. Mater. 17 (2005) 3904–3912.
[21] J. Geng, Z.P. Wu, W. Chen, L. Luo, J. Inorg. Mater. 175 (2) (2003) 480–484 (in Chinese).
[22] F. Clabau, X. Rocquefelte, S. Jobic, P. Deniard, M.-H. Whangbo, A. Glarcia, T. Le Mercier, Solid State Sci. 9 (2007) 608–612.